

its antiquark. The B meson's CP state is revealed by the subsequent decay of the neutral K. Its subscripts L and S, for *long* and *short*, denote the very disparate half-lives of the neutral kaon's two mass eigenstates.

In the example sketched in figure 1, at the moment of the first tagged B decay, the survivor must have been a B^0 . Its subsequent tagged demise, then, shows the transformation of a B^0 into a B_- after a time interval Δt of a few picoseconds, measured by Δz , the beam-direction component of the displacement between the two decay vertices in the detector.

If time-reversal symmetry holds, the transition rate, as a function of Δt , must precisely equal the rate for its

time reverse, $B_- \rightarrow B^0$. Figure 2 shows the results of the team's tests of that symmetry for four different neutral-B transformations. The data were gleaned from a few thousand appropriately tagged decays of neutral-B pairs.

The asymmetry parameter A , plotted as a function of Δt in each of the figure 2 panels, is defined as the difference between the rates of the transition and its time reverse, divided by their sum. Even in the absence of any T -symmetry violation, instrumental effects would cause the small departures of the measured A from zero indicated by the blue curves. But the best global fit to the actual data (red curves) constitutes a 14-standard-deviation

departure from the null hypothesis that T symmetry is not violated.

The level of T violation indicated by that fit agrees well with what one expects from inviolate CPT symmetry, given the well-characterized violation of CP symmetry in the neutral-B system. Indeed, the BaBar data also yield several direct tests of CPT symmetry. And none of them shows any evidence of its violation.

Bertram Schwarzschild

References

1. L. Wolfenstein, *Phys. Rev. Lett.* **83**, 911 (1999); *Int. J. Mod. Phys.* **8**, 501 (1999).
2. J. P. Lees et al. (BaBar collaboration), *Phys. Rev. Lett.* (in press), available at <http://arxiv.org/abs/1207.5832>.

A new 3D microscopy tool in the geologist's kit

Coherent Raman scattering can be exploited to image a rock's interior with molecular contrast.

In 1999 Sunney Xie and coworkers at Pacific Northwest National Laboratory published an article containing an image of three cervical cancer cells, in which each cell's mitochondria appear as bright yellow splotches in a sea of red cytoplasm.¹ The researchers used no fluorescent labels or stains to generate the color contrast; rather, they used a technique known as coherent anti-Stokes Raman scattering (CARS) microscopy.

The technique was developed in the early 1980s at the US Naval Research Laboratory, but it went virtually unnoticed until Xie and colleagues rediscovered and refined it. In the past decade, CARS has stirred considerable interest among biologists, and now work by Robert Burruss (US Geological Survey), Aaron Slepukov (Trent University, Peterborough, Ontario), Albert Stolow, and Adrian Pegoraro (both at National Research Council Canada) suggests the technique could also prove useful to geoscientists.² Applied to translucent samples of sedimentary rock, CARS microscopy produced richly informative three-dimensional maps that could shed new light on geochemical and geophysical processes.

Coherent Raman scattering

In CARS microscopy, chemical contrast is generated with a pair of laser pulses—a pump pulse and a Stokes

pulse—whose frequencies ω_p and ω_s differ by the frequency ω_v of a molecular vibration of interest. As depicted in figure 1a, a pump photon excites the molecule to a virtual state and a Stokes photon stimulates an emission that leaves the molecule in a vibrationally excited state. When a second pump photon scatters off the vibrating molecule, it can emerge as a so-called anti-Stokes photon, which has blueshifted frequency $\omega_{as} = \omega_p + \omega_v$. By mapping the intensity of the blueshifted signal as a function of location in the sample, one can construct a 3D map of the molecule's spatial distribution.

Raman scattering is notoriously inefficient; it typically occurs just once in every million or so scattering events. Thus conventional, spontaneous Raman scattering techniques yield a frequency-shifted signal that can be difficult to distinguish from noise. However, if Raman scattering is stimulated with lasers, as it is in CARS, it yields a coherent, and therefore much more intense, signal.

Speedy CARS

To implement CARS using Xie and colleagues' method, one has to synchronize a pair of picosecond pulsed lasers. Then, to scan a spectrum of vibrational resonances, one must repeatedly retune the lasers' frequencies. Three years ago, Stolow and coworkers at the National

Research Council Canada devised a simpler, quicker strategy that involves just a single, femtosecond pulsed laser.³

As sketched in figure 1b, they split a laser beam into two arms, one of which is then redshifted—by way of a photonic crystal fiber and bandpass filter—for use as the lower-frequency Stokes beam. As with any laser, however, a decrease in pulse duration comes at the cost of an increase in bandwidth. So the femtosecond pulses should be thought of not as having specific frequencies ω_p and ω_s but as containing broad distributions of frequencies that are centered on those values. In fact, the pulse bandwidths can be tens of times broader than the spectral lines they are meant to detect. That presents a seeming conundrum: How does one tune the difference frequency of two pulses to achieve a spectral resolution exceeding that of the pulses themselves?

The trick was to use what are commonly known as chirped pulses. Using blocks of dispersive glass, each pulse is stretched in a way that temporally sorts its light according to frequency: A miniature observer who watches the chirped pulse go by would see its frequency grow linearly with time. Stolow likens it to a "piano run" in which every note is played in sequence, from low to high. To understand how the chirp facilitates fine-tuning of two pulses' difference frequency, imagine someone playing two piano runs, one with each hand. As long as each hand progresses at the

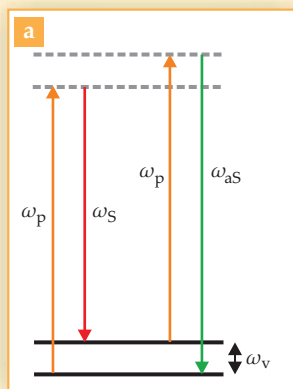
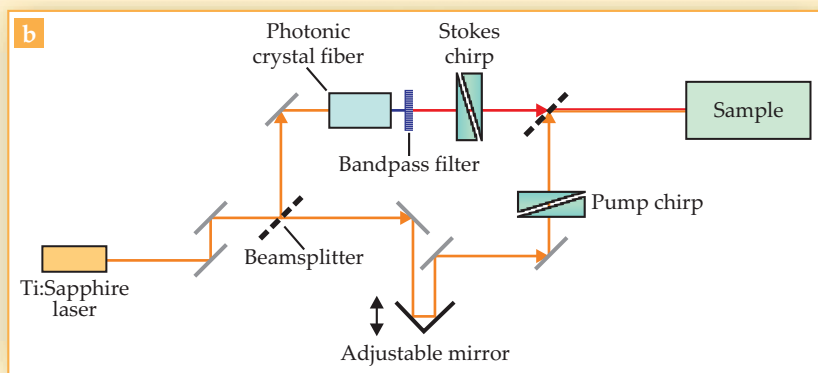


Figure 1. Coherent anti-Stokes Raman scattering.

(a) Energy-level diagram for CARS. A pump photon of frequency ω_p excites a molecule to a virtual state, and a Stokes photon of frequency ω_s stimulates an emission that leaves the molecule in a vibrationally excited state having frequency ω_v . When a pump photon inelastically scatters off the vibrating molecule, it emerges as an anti-Stokes photon of frequency $\omega_{as} = \omega_p + \omega_v$. **(b)** CARS microscopy can be implemented by splitting a single, femtosecond pulsed laser beam. A photonic-crystal fiber and bandpass filter impose a redshift in one arm, and an adjustable mirror imposes a time delay in the other. As described in the text, each pulse must be chirped—temporally stretched to separate different frequencies of light—to achieve the spectral resolution needed to probe vibrational resonances. (Adapted from ref. 4.)



same pace, it's possible to maintain a constant spacing of just a few keys between hands.

Analogously, Stolow and company fix the pulses' chirp rates so that a miniature observer who watches them pass would see a constant, and potentially quite narrow, frequency difference. That difference can then be retuned over a swath of spectrum by adjusting a mirror to alter the time delay between pulses; conveniently, there's no need to retune the lasers themselves.

Rocks in 3D

Even the most pristine mineral samples are flecked with tiny pockets of trapped liquid or gas known as fluid inclusions. Sometimes just microns in size and containing femtomoles of material, those inclusions help paint a picture of how Earth evolved over geological time scales; each inclusion amounts to a snapshot of the physical and chemical state of a particular part of Earth's crust at a particular moment in time. Interpreting the snapshot calls for identifying the inclusion's contents and its formation history; inclusions

can be trapped when a mineral precipitates out of the liquid phase, or they can form later on when a mineral fractures and heals.

On learning of Stolow's CARS microscopy technique, Burruss, a geochemist, thought it might be useful for imaging methane inside fluid inclusions. In theory, methane can be detected with conventional Raman scattering, but when an inclusion also contains long-chain hydrocarbons, the larger molecules' natural fluorescence tends to obscure methane's Raman spectral lines. That's particularly troubling for petroleum scientists, who need to know how methane is—and was—distributed in Earth's crust in order to unravel the processes responsible for generating fossil fuels.

Applying CARS microscopy to translucent samples of quartz, calcite, and hornblende, Burruss, Stolow, and company found they could easily identify methane and several other chemical constituents of microscopic inclusions, even when long-chain hydrocarbons were present. What's more, the intense femtosecond pulses also give rise to second harmonic

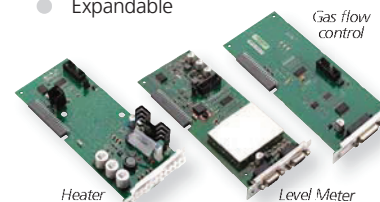
Mercury Temperature Controller / Magnet Power Supplies

Intelligent control of cryogenic and magnet systems



Top to bottom: **MercuryTC** temperature controller and **MercuryPS** magnet power supplies (master and slave units)

- Accurate - measures and controls temperatures down to 250 mK
- Expandable



- Stable and configurable magnet power supplies including multi-axis magnet control
- User-friendly touch screen interface and remote system control with the Oxsoft IDK software



For further information:
mercury@oxinst.com
www.oxinst.com/mercury
 and view our new Mercury video.



The Business of Science®

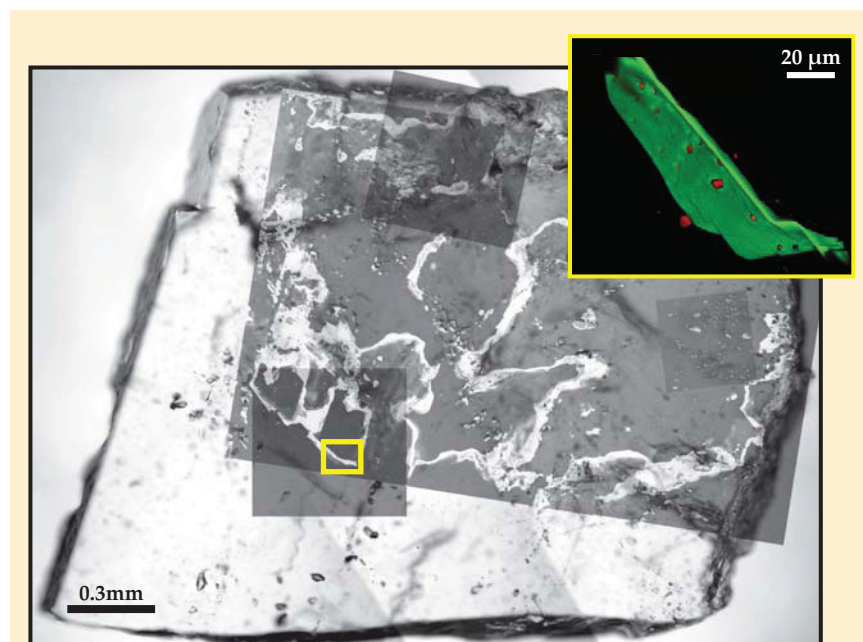


Figure 2. A quartz sample contains more than meets the eye. Superimposed on this microscope image are four images (the dark rectangular frames) produced by detecting a frequency-doubling effect known as second harmonic generation. The SHG images reveal the sample's internal web of facets and fractures. In the inset—which corresponds to the area outlined in yellow—the SHG signal (green) reveals a microfracture and the coherent anti-Stokes Raman scattering signal (red) reveals pockets of trapped methane. (Image courtesy of Robert Burruss; inset adapted from ref. 2.)

generation (SHG): At interfaces within the material, occasionally two photons of frequency ω_p are converted to one photon of frequency $2\omega_p$. By mapping

spatial variations in that frequency-doubled signal, the team could construct images of a sample's internal microstructure.

Figure 2 shows four SHG images of a quartz sample superimposed on a conventional microscope image. The SHG images reveal inclusion walls, microfractures, grain boundaries, and other microstructures. Paired with CARS, an SHG image allows one to determine not just the contents of an inclusion, but also whether the inclusion is associated with a particular fracture event. For example, the composite SHG–CARS image in figure 2 shows methane-rich inclusions embedded along a healed microfracture.

Burruss envisions several new applications for CARS microscopy, including visualizing how different minerals and crystalline domains intermingle inside rocks. Broadly speaking, he draws an analogy with atomic force microscopy: “When geoscientists first found out about AFM, they said, ‘Wow! This could be really useful for learning about minerals,’ and now AFM techniques are used extensively in the geosciences. I think there’s a similar opportunity with CARS.”

Ashley G. Smart

References

1. A. Zumbusch, G. R. Holtom, X. S. Xie, *Phys. Rev. Lett.* **82**, 4142 (1999).
2. R. C. Burruss et al., *Geology* (in press).
3. A. F. Pegoraro et al., *Opt. Express* **17**, 2984 (2009).
4. A. F. Pegoraro et al., *BioPhotonics*, October 2009, p. 36.

physics update

These items, with supplementary material, first appeared at <http://www.physicstoday.org>.

A single-atom qubit in silicon. The up or down spin of an electron makes it a natural qubit to use in an eventual quantum computer. One difficulty in any qubit system is preserving the qubits' fragile phase coherence long enough to perform a sequence of quantum calculations. Another is scalability. For instance, qubits made from isolated atoms offer long coherence times but are hard to scale up into macroscopic devices, whereas those made from bulk semiconductors are scalable but usually suffer from high decoherence rates (see *PHYSICS TODAY*, March 2006, page 16). A research group led by Andrea Morello and Andrew Dzurak (both from the University of New South Wales in Australia) have now combined the advantages of both architectures by fabricating a qubit based on a single atom's electron spin. Ordinarily, a phosphorus atom embedded in silicon donates an electron that enhances Si's electrical conductivity, but at cryogenic temperatures the electron becomes trapped around the P nucleus. The qubit formed by the spin of the electron is protected from decoherence thanks to weak spin-orbit coupling and a near absence of nuclear spin in the surrounding Si lat-

tice. After implanting P in a Si chip, the researchers also fashioned on the chip a transistor to initialize and read out the qubit's spin state. Between those operations they used microwave pulses resonant with the spin transition frequency to coherently manipulate the qubit's state over about 200 μ s; that's long enough to enable more than 1000 qubit operations. (J. J. Pla et al., *Nature* **489**, 541, 2012.) —RMW

Interacting solitary waves. Ever since John Scott Russell first reported a large, long-lived, solitary wave of constant shape on a Scottish canal in 1834, such waves have been an active area of research in diverse fields that include not only oceanography but also optics, cosmology, plasma physics, and even biophysics. Dubbed solitons, solitary waves are inherently nonlinear, and their velocities depend on amplitude. When two collide in one dimension, they can appear to bounce off each other or to have the faster one jump over the slower one. In 2D, even more complex interactions can occur. Mark Ablowitz and Douglas Baldwin of the University of Colorado Boulder report observing surprisingly frequent, varied nonlinear interactions between multiple solitary water waves at two flat beaches; the photo is an example of the aptly named “Y-type” interaction. (Additional photos and videos of